Cos 2ϕ asymmetry in J/ψ and jet production at the EIC and effect of TMD evolution

Asmita Mukherjee

IIT Bombay, Mumbai, India

Sar Wors 2025 : 4 th Sardinian Workshop on Spin

Collinear pdfs : nucleon structure In 1-D

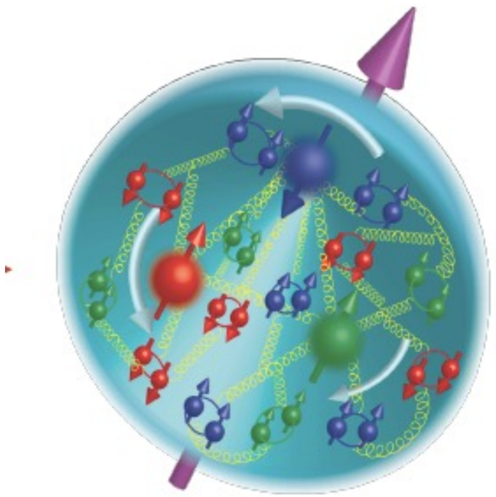

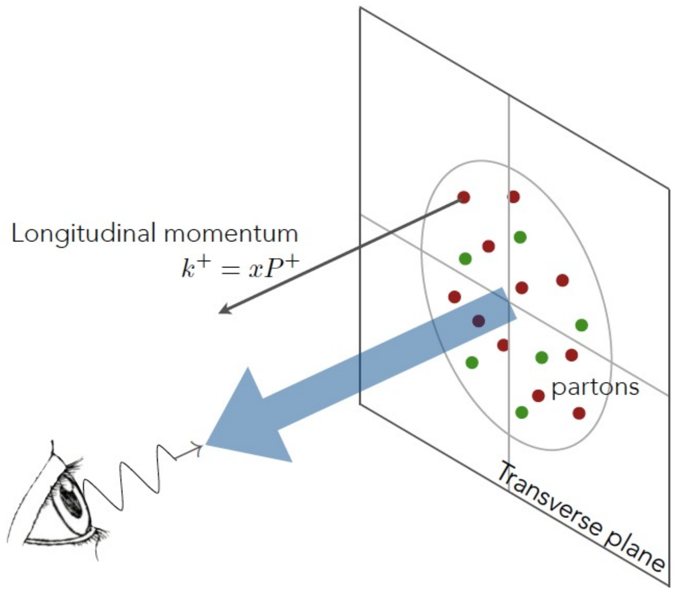

Probed in deep inelastic scattering

Motion of quarks in the transverse plane ignored

Non-perturbative : Is extracted by fitting
experimental data

Independent of process : once extracted can be used to predict cross section of another process as the scale evolution is known

One can also perform a polarized scattering experiment : probes polarized structure functions

Transverse momentum dependent parton distributions (TMDs)

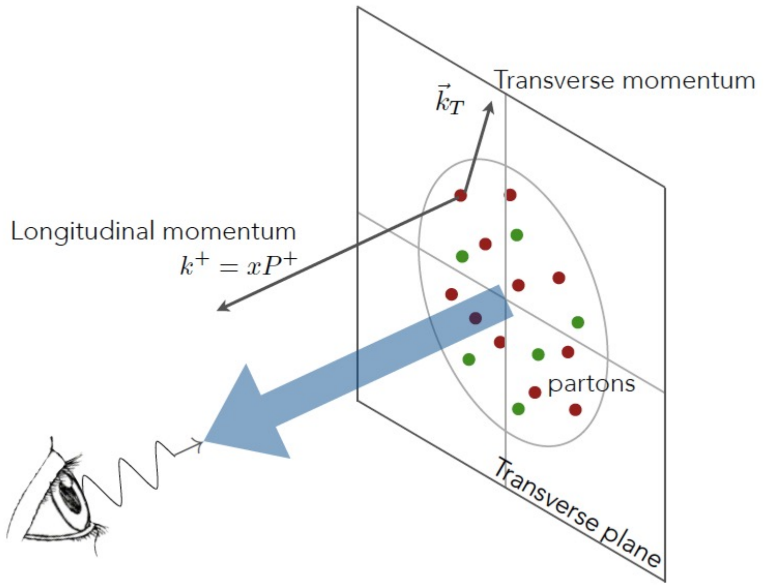

Large (30-40%) Single transverse spin asymmetries were seen at FermiLab and RHIC experiments

Such large asymmetries cannot be explained in terms of collinear leading twist pdfs : need TMDs, or twist three pdfs

$$A_N = \frac{d\sigma^\uparrow - d\sigma^\downarrow}{d\sigma^\uparrow + d\sigma^\downarrow}$$

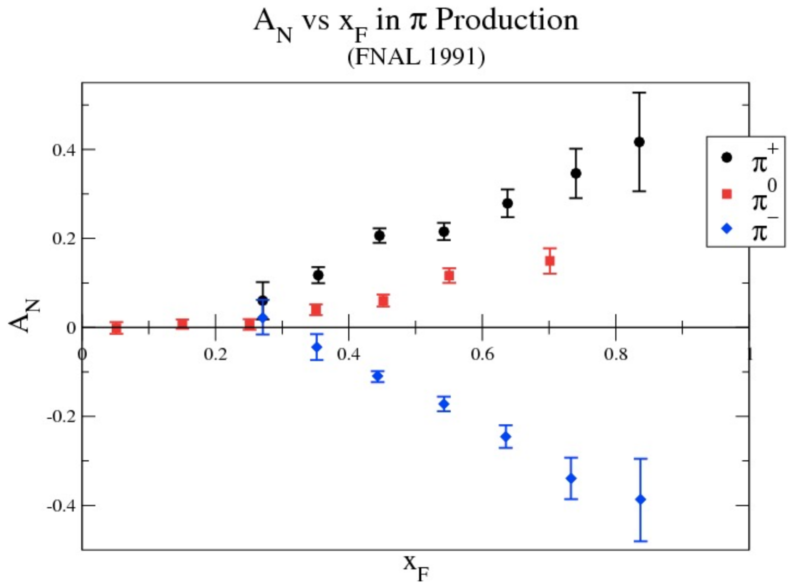

TMDs : functions of x and intrinsic transverse momentum : Gives a 3 D picture of the nucleon in momentum space, process dependent

Correlations of spin, OAM and k_T : in terms of TMDs

QUARK TMD

QUARKS	*unpolarized*	*chiral*	*transverse*
U	f_1		$h_1^{\perp}$
L		g_{1L}	$h_{1L}^{\perp}$
T	$f_{1T}^{\perp}$	g_{1T}	$h_{1T}, h_{1T}^{\perp}$

Angeles-Martinez *et al.*, Acta Phys, Pol. B46 (2015)
Mulders, Rodrigues, PRD 63 (2001)
Meissner, Metz, Goeke, PRD 76 (2007)

There are eight quark TMDs at leading twist

Only three of them survive after transverse momentum integration

Two TMDs, Sivers function and Boer-Mulders function are odd under time reversal

TMDs contribute in different azimuthal angle asymmetries

Pavia 2017, JHEP 06 (2017)
Scimemi, Vladimirov, JHEP 06 (2020)
MAP Collaboration, JHEP (2022)

Bury, Prokudin, Vladimirov, PRL 126 (2021)
Echevarria, Kang, Terry, JHEP 01 (2021)
Bacchetta, Delcarro, Pisano, Radici, CP, PLB 827 (2022)

Gluon TMDs

GLUONS	*unpolarized*	*circular*	*linear*
U	f_1^g		$h_1^{\perp g}$
L		g_{1L}^g	$h_{1L}^{\perp g}$
T	$f_{1T}^{\perp g}$	g_{1T}^g	$h_{1T}^g,\ h_{1T}^{\perp g}$

Angeles-Martinez *et al.*, Acta Phys, Pol. B46 (2015)
Mulders, Rodrigues, PRD 63 (2001)
Meissner, Metz, Goeke, PRD 76 (2007)

$h_1^{\perp g}$: Linearly polarized gluon distribution in unpolarized hadron; T even

$f_{1T}^{\perp g}$ Gluon Sivers function in Transversely polarized proton

$$h_1^g \equiv h_{1T}^g + \frac{\boldsymbol{p}_T^2}{2M_p^2} h_{1T}^{\perp g}$$

Vanish under p_T integration

In contrast to quark TMDs, very little is known about gluon TMDs

$$\Gamma^{[\mathcal{U},\mathcal{U}']\mu\nu} \propto \langle P,S|\,\mathrm{Tr_c}\big[\,F^{+\nu}(0)\,\mathcal{U}^{\mathcal{C}}_{[0,\xi]}\,F^{+\mu}(\xi)\,\mathcal{U}^{\mathcal{C}'}_{[\xi,0]}\,\big]\,|P,S\rangle$$

Gluon TMDs need two gauge links for gauge invariance

Mulders, Rodrigues, PRD 63 (2001)
Buffing, Mukherjee, Mulders, PRD 88 (2013)
Boer, Cotogno, Van Daal, Mulders, Signori, Zhou, JHEP 1610 (2016)

Linearly polarized Gluon distributions

Linearly polarized gluon distributions were first introduced in

Mulders and Rodrigues, PRD 63, 094021 (2001)

Operator structure of unintegrated gluon distributions can be different in different processes. In the literature, at small x, Weizsacker-Williams (WW) gluon distribution contains both past or both future pointing gauge links and dipole distributions contain one past and one future pointing gauge link. These are also called f and d type distributions, contribute in different processes. Extensive literature on unintegrated gluon distributions.

Linearly polarized gluon TMD : Measures an interference between an amplitude when the active gluon is polarized along x (or y) direction and a complex conjugate amplitude with the gluon polarized in y (or x) direction in an unpolarized hadron

Affects unpolarized cross section as well as generates a $\cos 2\phi$ asymmetry

Gluon TMDs in J/ψ production processes

Semi-inclusive J/ψ production in eP collision is a good channel to probe gluon TMDs

Godbole, Misra, AM, Rawoot, PRD (2012); AM and Rajesh EPJC (2017)

For low transverse momentum region, TMD factorization is expected to hold and for large transverse momentum collinear factorization is applicable. In the intermediate region, results from these two formalisms should match

TMD factorized description of the process needs smearing effects to be taken into account in the form of TMD shape functions. The perturbative tail of the shape function can be obtained through a matching procedure.

M. G. Echevarria, JHEP (2019), Boer et al, JHEP (2023)

Also gluon TMDs can be probed in back-to-back production of J/ψ and photon/jet/pion, TMD factorization is expected to be valid. The small scale is provided by the transverse momentum of the pair. By varying the invariant mass of the pair scale evolution of the TMDs can be studied

So far the smearing effects and the shape functions are not calculated by matching procedure

Production of J/ψ in NRQCD

In NRQCD the heavy quark pair is produced in the hard process either in color octet or in color singlet configuration

Then they hadronize to form a color singlet quarkonium state of given quantum numbers through soft gluon emission

Hard process is calculated perturbatively and soft process is given in terms of long distance matrix elements (LDMEs) that are determined from data

The LDMEs are categorized by performing an expansion in terms of the relative velocity of the heavy quark v in the limit $v \ll 1$

The theoretical predictions are arranged as double expansions in terms of v as well as α_s.

C. E. Carlson and R. Suaya, Phys. Rev. D 14, 3115 (1976).
E. L. Berger and D. L. Jones, Phys. Rev. D 23, 1521 (1981).
R. Baier and R. Ruckl, Phys. Lett. B 102B, 364 (1981).
R. Baier and R. Ruckl, Nucl. Phys. B201, 1 (1982).
E. Braaten and S. Fleming, Phys. Rev. Lett. 74, 3327 (1995).
P. L. Cho and A. K. Leibovich, Phys. Rev. D 53, 150 (1996).

G. T. Bodwin, E. Braaten, and G. P. Lepage, Phys. Rev. D 51, 1125 (1995); 55, 5853(E) (1997).

Production of J/ψ in NRQCD

J/ψ is a bound state of charm quark and anti-quark ($Q\bar{Q}$)

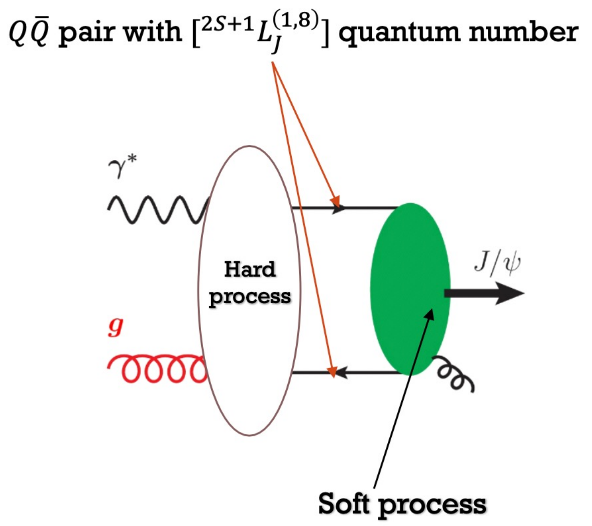

Long distance matrix elements (LDMEs) : Describes hadronization of of $Q\bar{Q}[n]$ states into final quarkonium state

NRQCD factorization

$$d\sigma^{ab\to J/\psi} = \sum_n d\hat{\sigma}[ab \to c\bar{c}(n)]\langle 0 \mid \mathcal{O}_n^{J/\psi} \mid 0\rangle$$

Perturbative short distance coefficient

G. T. Bodwin et al, PRD51 (1995), Lepage 95

Subprocess cross section for formation of heavy quark pair in particular color, angular momentum and spin state "n" : $^{2S+1}L_J$, calculated by perturbative QCD

Cos 2ϕ asymmetry in almost back-to-back production of J/ψ and jet in ep collision

$$e(l) + p(P) \rightarrow e(l') + J/\psi(P_\psi) + jet(P_j) + X$$

$$Q^2 = -q^2, \qquad s = (P+l)^2, \qquad W^2 = (P+q)^2,$$

$$x_B = \frac{Q^2}{2P\cdot q}, \qquad y = \frac{P\cdot q}{P\cdot l}, \qquad z = \frac{P\cdot P_\psi}{P\cdot q}.$$

z<1 : energy fraction of the virtual photon carried by the hadron in proton rest frame

Use TMD factorization in the kinematics where the outgoing J/ψ and (gluon) jet are almost back-to back

$$\mathbf{q}_t \equiv \mathbf{P}_{\psi\perp} + \mathbf{P}_{j\perp}, \qquad \mathbf{K}_t \equiv \frac{\mathbf{P}_{\psi\perp} - \mathbf{P}_{j\perp}}{2}.$$

$$|\mathbf{q}_t| \ll |\mathbf{K}_t|.$$

Use NRQCD to calculate the J/ψ production

Also compare with the color singlet (CS) model result

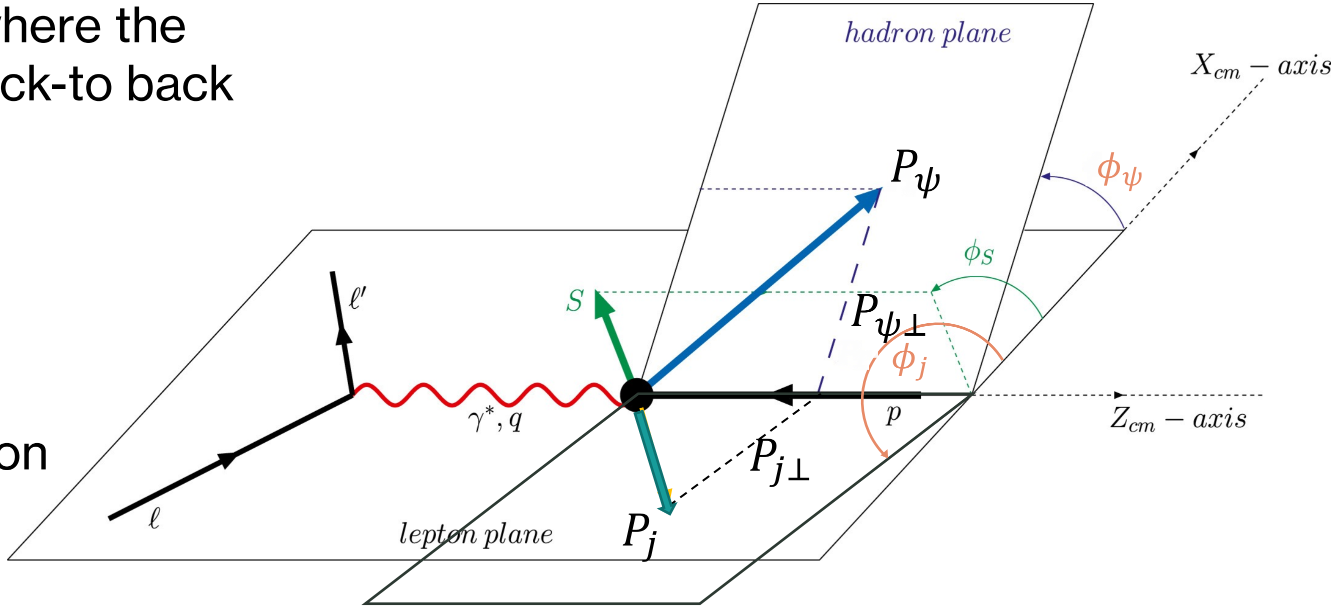

$\gamma^* - p$ c.o.m frame

J/ψ and jet in ep collision : Diagrams

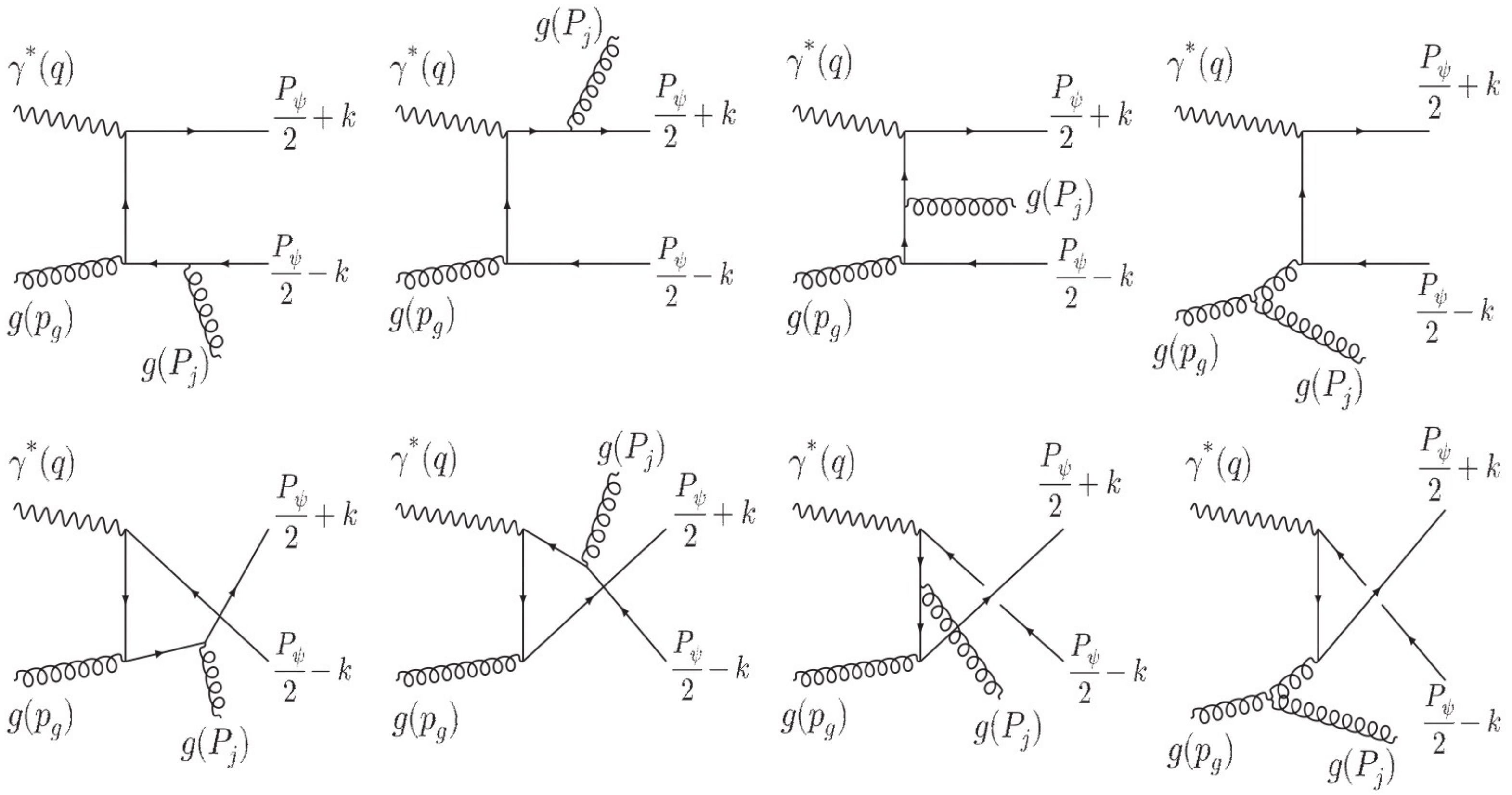

FIG. 1. Feynman diagrams for the partonic process $\gamma^*(q) + g(p_g) \to J/\psi(\mathrm{P}_\psi) + g(\mathrm{P}_j)$.

Calculation of amplitude using NRQCD

The amplitude can be written as

D. Boer and C. Pisano , PRD (2012)

$$M(\gamma^* g \to Q\bar{Q}[^{2S+1}L_J^{(1,8)}](P_\psi) + g)$$
$$= \sum_{L_z S_z} \int \frac{d^3k}{(2\pi)^3} \Psi_{LL_z}(k) \langle LL_z ; SS_z | JJ_z \rangle \mathrm{Tr}[\mathcal{O}(q, p, P_\psi, k) \mathcal{P}_{SS_z}(P_\psi, k)]$$

Amplitude for production of $Q\bar{Q}$ pair : $\mathcal{O}(q, p, P_\psi, k) = \sum_{m=1}^{8} C_m \mathcal{O}_m(q, p, P_\psi, k)$

The spin projection operator, $\mathcal{P}_{SS_z}(P_\psi, k)$, projects the spin triplet and spin singlet states of $Q\bar{Q}$ pair

$$\mathcal{P}_{SS_z}(P_\psi, k) = \sum_{s_1 s_2} \left\langle \frac{1}{2} s_1 ; \frac{1}{2} s_2 \middle| SS_z \right\rangle v\left(\frac{P_\psi}{2} - k, s_1\right) \bar{u}\left(\frac{P_\psi}{2} + k, s_2\right)$$
$$= \frac{1}{4M_\psi^{3/2}} (-P_\psi + 2k + M_\psi) \Pi_{SS_z} (P_\psi + 2k + M_\psi) + O(k^2)$$

$\Pi_{SS_z} = \gamma^5$ for spin singlet ($S = 0$)

$\Pi_{SS_z} = \epsilon^{\mu}_{S_z}(P_\psi)\gamma_\mu$ for spin triplet ($S = 1$)

Almost back-to-back production of J/ψ and jet

$$
\begin{aligned}
d\sigma = & \frac{1}{2s}\frac{d^3 l'}{(2\pi)^3 2E_{l'}}\frac{d^3 \mathrm{P}_\psi}{2E_\psi(2\pi)^3}\frac{d^3 \mathrm{P}_j}{2E_j(2\pi)^3} \\
& \times \int dx d^2\mathbf{p}_T (2\pi)^4 \delta^4(q+p_g-\mathrm{P}_j-\mathrm{P}_\psi) \\
& \times \frac{1}{Q^4} L^{\mu\mu'}(l,q)\Phi_g^{\nu\nu'}(x,\mathbf{p}_T^2)\mathcal{M}_{\mu\nu}^{g\gamma^*\to J/\psi g}\mathcal{M}_{\mu'\nu'}^{*g\gamma^*\to J/\psi g}.
\end{aligned}
$$

$$
\begin{aligned}
& \mathcal{M}(\gamma^* g \to Q\bar{Q}[^{2S+1}L_J^{(1,8)}]g) \\
& = \sum_{L_z S_z}\int \frac{d^3\mathbf{k}}{(2\pi)^3}\Psi_{LL_z}(\mathbf{k})\langle LL_z; SS_z|JJ_z\rangle \\
& \times \mathrm{Tr}[O(q,p_g,\mathrm{P}_\psi,k)\mathcal{P}_{SS_z}(\mathrm{P}_\psi,k)],
\end{aligned}
$$

Contribution comes from the color singlet state $({}^3S_1^{(1)})$ and color octet states $({}^3S_1^{(8)}, {}^1S_0^{(8)}, {}^3P_{J(0,1,2)}^{(8)})$

In NRQCD, k, the relative momentum of the charm quark is small.
We have Taylor expanded the amplitude about k=0. The first term gives the S wave contribution and second term the p wave contribution

Formation of the bound state J/ψ from the heavy quark pair is encoded in the non-perturbative long distance matrix elements (LDMEs). These are obtained by fitting data

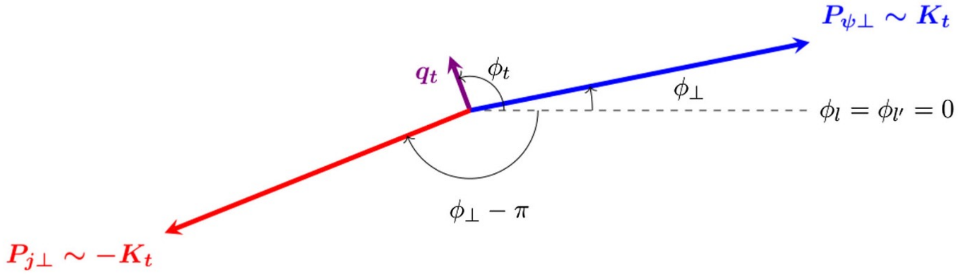

Upper bound of the asymmetries : U. D'Alesio, F. Murgia, C. Pisano, and P. Taels *Phys.Rev.D* 100 (2019) 9, 094016

Asymmetry

$$\langle\cos 2\phi_t\rangle \equiv A^{\cos 2\phi_t} = \frac{\int \mathrm{q}_t \mathrm{d}\mathrm{q}_t \frac{\mathbf{q}_t^2}{M_p^2}\mathbb{B}_0 h_1^{\perp g}(x,\mathbf{q}_t^2)}{\int \mathrm{q}_t \mathrm{d}\mathrm{q}_t \mathbb{A}_0 f_1^g(x,\mathbf{q}_t^2)}.$$

$$\frac{d\sigma}{dz\,dy\,dx_B\,d^2\mathbf{q}_t\,d^2\mathbf{K}_t} = \frac{1}{(2\pi)^4}\frac{1}{16sz(1-z)Q^4}\Big\{(\mathbb{A}_0 + \mathbb{A}_1\cos\phi_\perp + \mathbb{A}_2\cos 2\phi_\perp)f_1^g(x,\mathbf{q}_t^2)$$
$$+\frac{\mathbf{q}_t^2}{M_P^2}h_1^{\perp g}(x,\mathbf{q}_t^2)(\mathbb{B}_0\cos 2\phi_t + \mathbb{B}_1\cos(2\phi_t-\phi_\perp) + \mathbb{B}_2\cos 2(\phi_t-\phi_\perp)$$
$$+\mathbb{B}_3\cos(2\phi_t-3\phi_\perp) + \mathbb{B}_4\cos(2\phi_t-4\phi_\perp))\Big\}.$$

Gaussian parametrization of TMDs :

$$f_1^g(x,\mathbf{q}_t^2) = f_1^g(x,\mu)\frac{1}{\pi\langle\mathbf{q}_t^2\rangle}e^{-\mathbf{q}_t^2/\langle\mathbf{q}_t^2\rangle},$$

$$h_1^{\perp g}(x,\mathbf{q}_t^2) = \frac{M_p^2 f_1^g(x,\mu)}{\pi\langle\mathbf{q}_t^2\rangle^2}\frac{2(1-r)}{r}e^{1-\frac{\mathbf{q}_t^2}{r\langle\mathbf{q}_t^2\rangle}},$$

Boer and Pisano, PRD, 2012

$\langle\mathbf{q}_t^2\rangle = 0.25\ \mathrm{GeV}^2.$ r=1/3

Spectator model :

$$F^g(x,\mathbf{q}_t^2) = \int_M^\infty dM_X\rho_X(M_X)\hat{F}^g(x,\mathbf{q}_t^2;M_X).$$

Spectral function

$$\rho_X(M_X) = \mu^{2a}\left[\frac{A}{B+\mu^{2b}} + \frac{C}{\pi\sigma}e^{-\frac{(M_X-D)^2}{\sigma^2}}\right],$$

$$\hat{f}_1^g(x,\mathbf{q}_t^2;M_X) = -\frac{1}{2}g^{ij}[\Phi^{ij}(x,\mathbf{q}_t,S)+\Phi^{ij}(x,\mathbf{q}_t,-S)]$$
$$= [(2Mxg_1 - x(M+M_X)g_2)^2[(M_X-M(1-x))^2+\mathbf{q}_t^2]$$
$$+2\mathbf{q}_t^2(\mathbf{q}_t^2+xM_X^2)g_2^2 + 2\mathbf{q}_t^2M^2(1-x)(4g_1^2-xg_2^2)][(2\pi)^3 4xM^2(L_X^2(0)+\mathbf{q}_t^2)^2]^{-1},$$

$$\hat{h}_1^{\perp g}(x,\mathbf{q}_t^2;M_X) = \frac{M^2}{\varepsilon_t^{ij}\delta^{jm}(p_t^j p_t^m + g^{jm}\mathbf{q}_t^2)}\varepsilon_t^{ln}\delta^{nr}[\Phi^{nr}(x,\mathbf{q}_t,S)+\Phi^{nr}(x,\mathbf{q}_t,-S)]$$
$$= [4M^2(1-x)g_1^2 + (L_X^2(0)+\mathbf{q}_t^2)g_2^2]\times[(2\pi)^3x(L_X^2(0)+\mathbf{q}_t^2)^2]^{-1}.$$

A. Bacchetta, F. G. Celiberto, M. Radici, and P. Taels, Eur. Phys. J. C 80, 733 (2020).

TMD Evolution

Also incorportated TMD evolution in the asymmetry

Aybat and Rogers, PRD 83, 114042 (2011)

TMD evolution is done in impact parameter space

S_A and S_{np} are perturbative and non-perturbative Sudakov factors

$$\hat{f}(x, \mathbf{b}_t^2, Q_f^2) = \frac{1}{2\pi} \sum_{p=q,\bar{q},g} (C_{g/p} \otimes f_1^p)(x, Q_i^2) \times e^{-\frac{1}{2}S_A(\mathbf{b}_t^2, Q_f^2, Q_i^2)} e^{-S_{np}(\mathbf{b}_t^2, Q_f^2)},$$

$$S_A(\mathbf{b}_t^2, Q_f^2, Q_i^2) = \frac{C_A}{\pi} \int_{Q_i^2}^{Q_f^2} \frac{d\eta^2}{\eta^2} \alpha_s(\eta) \left(\log\frac{Q_f^2}{\eta^2} - \frac{11 - 2n_f/C_A}{6} \right)$$

$$= \frac{C_A}{\pi} \alpha_s \left(\frac{1}{2} \log^2 \frac{Q_f^2}{Q_i^2} - \frac{11 - 2n_f/C_A}{6} \log \frac{Q_f^2}{Q_i^2} \right).$$

$$S_{np} = \frac{A}{2} \log\left(\frac{Q_f}{Q_{np}}\right) \mathrm{b}_c^2, \qquad Q_{np} = 1 \text{ GeV}.$$

Scarpa, Boer, Echevarria, Lansberg, Pisano, Schlegel, EPJC(2020)

Boer, D'Alesio, Murgia, Pisano, and Taels, JHEP (2020) 40.

$$Q_f = \sqrt{M_\psi^2 + \mathrm{K}_t^2}. \qquad A = 2.3 \text{ GeV}^2$$

$$Q_i = 2e^{-\gamma_E}/\mathrm{b}_t$$

Used b_{t*} prescription to prevent Q_i larger than Q_f for low b_t

Final expressions are :

$$f_1^g(x, \mathbf{q}_t^2) = \frac{1}{2\pi} \int_0^\infty \mathrm{b}_t d\mathrm{b}_t J_0(\mathrm{b}_t \mathrm{q}_t) \left\{ f_1^g(x, Q_f^2) - \frac{\alpha_s}{2\pi} \left[\left(\frac{C_A}{2} \log^2 \frac{Q_f^2}{Q_i^2} - \frac{11C_A - 2n_f}{6} \log \frac{Q_f^2}{Q_i^2} \right) f_1^g(x, Q_f^2) + (P_{gg} \otimes f_1^g + P_{gi} \otimes f_1^i)(x, Q_f^2) \log \frac{Q_f^2}{Q_i^2} - 2 f_1^g(x, Q_f^2) \right] \right\} \times e^{-S_{np}(\mathbf{b}_t^2)}.$$

$$\frac{\mathbf{q}_t^2}{M_p^2} h_1^{\perp g(2)}(x, \mathbf{q}_t^2) = \frac{\alpha_s}{\pi^2} \int_0^\infty d\mathrm{b}_t \mathrm{b}_t J_2(\mathrm{q}_t \mathrm{b}_t) \left[C_A \int_x^1 \frac{d\hat{x}}{\hat{x}} \left(\frac{\hat{x}}{x} - 1 \right) f_1^g(\hat{x}, Q_f^2) + C_F \sum_{p=q,\bar{q}} \int_x^1 \frac{d\hat{x}}{\hat{x}} \left(\frac{\hat{x}}{x} - 1 \right) f_1^p(\hat{x}, Q_f^2) \right] \times e^{-S_{np}(\mathbf{b}_t{}^2)}.$$

Numerical estimate of the asymmetry

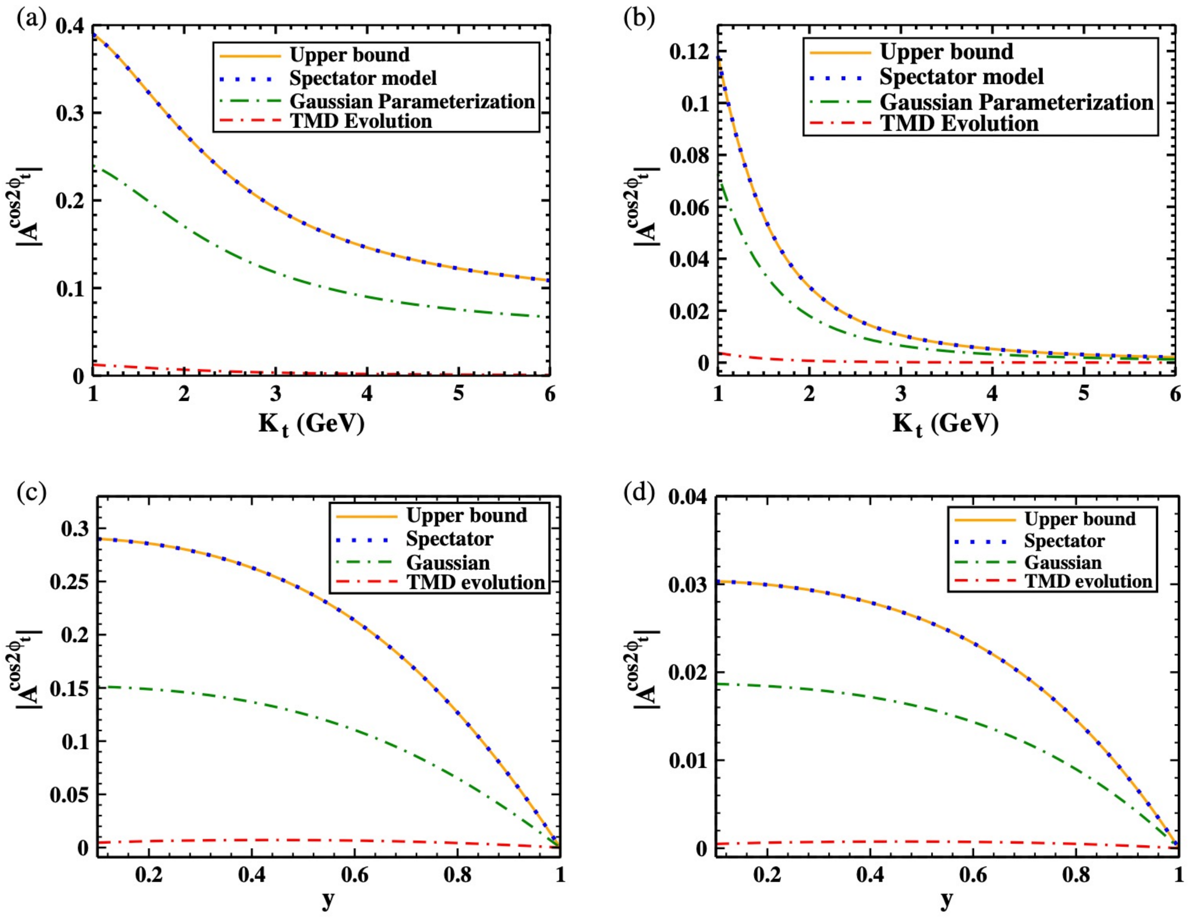

NRQCD

CS

$y = 0.3$ In upper panels $\sqrt{s} = 140\ GeV$

$K_t = 0.2\ GeV$ In lower panels

Result in spectator model in the kinematics considered overlaps with the upper bound saturating the positivity bound

Result is Gaussian parametrization lower than in spectator model

Asymmetries in CS smaller than in NRQCD

Raj Kishore, AM, Amol Pawar, M. Siddiqah, *Phys.Rev.D* 106 (2022) 3, 034009

TMD evolution

In impact parameter space, the perturbative part of the TMDs evolved from initial to final scale can be written as

$$\hat{F}(x, b_T, \zeta, \mu) = e^{-\frac{1}{2}S_A(b_T;\zeta,\zeta_0,\mu,\mu_0)}\hat{F}(x, b_T, \zeta_0, \mu_0)$$

Aybat and Rogers (2011)

S_A the perturbative Sudakov factor that resums large UV and rapidity logs : same for unpolarized and polarized TMD valid in the perturbative domain: $|b_T| \ll 1/\Lambda_{QCD}$

$$S_A(\mathbf{b}_t^2, Q_f^2, Q_i^2) = \frac{C_A}{\pi}\int_{Q_i^2}^{Q_f^2}\frac{d\eta^2}{\eta^2}\alpha_s(\eta)\left(\log\frac{Q_f^2}{\eta^2} - \frac{11-2n_f/C_A}{6}\right)$$
$$= \frac{C_A}{\pi}\alpha_s\left(\frac{1}{2}\log^2\frac{Q_f^2}{Q_i^2} - \frac{11-2n_f/C_A}{6}\log\frac{Q_f^2}{Q_i^2}\right).$$

For $b_T \ll \Lambda_{QCD}^{-1}$, perturbative tails of TMDs at the initial scale can be expressed by OPE:

$$\hat{F}_{g/A}(x, b_T, \mu_0, \zeta_0) = \sum_{j=q,\bar{q},g} C_{g/j}(x, b_T; \mu_0, \zeta_0) \otimes f_{j/A}(\hat{x}, \mu_0)$$

Perturbative Wilson coeffs are dependent on specific TMD

Collinear pdfs

Holds in small b_T region

TMD evolution

Wilson coefficients can be expanded in powers of α_S as

$$C_{g/a}(x;\mu_b^2) = \delta_{ga}\delta(1-x) + \sum_{k=1}^{\infty} C_{g/a}^{k}(x)\left(\frac{\alpha_S(\mu_b)}{\pi}\right)^k$$

We need to introduce a non-perturbative Sudakov factor that freezes the perturbative contribution slowly as b_T gets larger.

$$\hat{F}(x,b_T,\zeta,\mu) = e^{-\frac{1}{2}S_A(b_T^*;\zeta,\zeta_0,\mu,\mu_0)}\hat{F}(x,b_T^*,\zeta_0,\mu_0)e^{-S_{NP}(x,b_T)}$$

Fourier transform needs entire b_T region. But applicability of the perturbative expression confined in the range $b_0/Q < b_T < b_{T_{\max}}$.

For small b_T region μ_b exceeds hard scale, so evolution should stop.

TMD evolution

$$b_T^*(b_c(b_T)) = \frac{b_c(b_T)}{\sqrt{1 + \left(\frac{b_c(b_T)}{b_{T_{\max}}}\right)^2}}, \qquad b_c(b_T) = \sqrt{b_T^2 + \left(\frac{b_0}{Q}\right)^2}. \qquad b_{T_{\max}} = 1.5\ \mathrm{GeV}^{-1}.$$

This ensures that $\mu_{b^*} = \frac{b_0}{b_T^*(b_c)}$ Always lies between Q and $b_0/b_{T_{\max}}$ When b_T tends to 0 and infinity respectively

Non-perturbative factor suppresses the perturbative contribution for large b_T, should be equal to 1 for small b_T, for large b_T should decrease monotonically to zero typically within the confinement distance.

Result of TMD evolution cannot be uniquely predicted until the non-perturbative part is extracted from the data : plays an important role in the evolution. Different ansatz exist constrained by the above conditions.

Non-perturbative factor (gluon TMD)

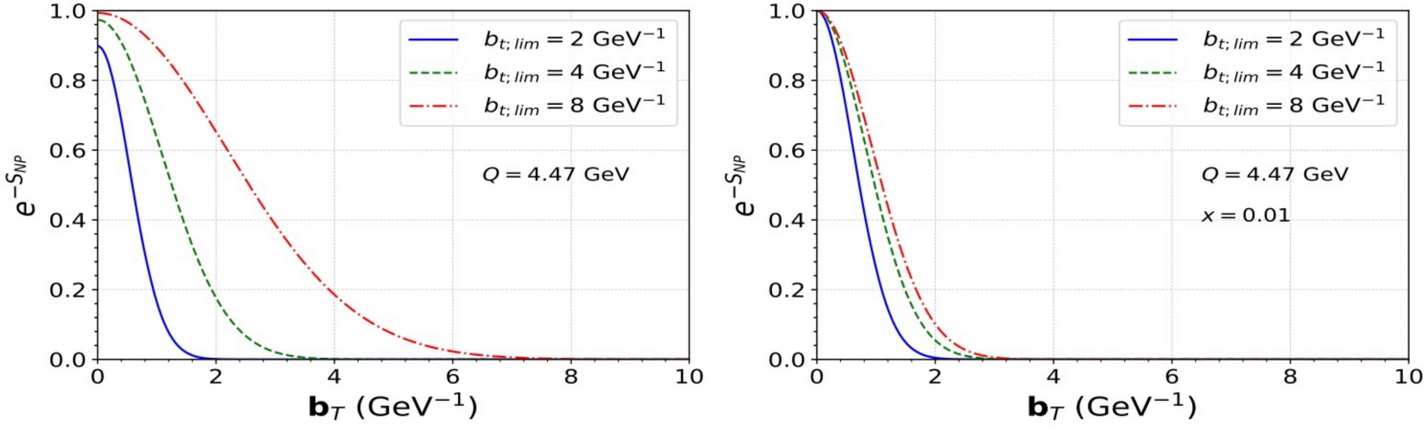

(a) (b)

$b_{t;\text{lim}}$ Defined from the non-pert factor such that exp(-S_{NP}) becomes negligible at a distance

A controls the width of the nonperturbative Sudakov factor for a particular Q. Obtained at $b_T = b_{T,\text{ lim}}$

TABLE I. Value of parameter A used in $e^{-S_{NP}}$ evaluated at $Q = 4.47$ GeV.

A (GeV^2)	$b_{t;\text{lim}}$ (GeV^{-1})	r (fm)
2.2697727	2	0.2
0.57415574	4	0.4
0.14395514	8	0.8

(a) $$S_{NP}(b_c(b_T)) = \frac{A}{2}\ln\left(\frac{Q}{Q_{NP}}\right)b_c^2(b_T), \qquad Q_{NP} = 1\text{ GeV}.$$

Scarpa, Boer, Echevarria, Lansberg, Pisano, Schlegel, Eur. Phys. J. C 80, 87 (2020).

TABLE II. Values of the parameters A and B used in $e^{-S_{NP}}$ evaluated at $Q = 12$ GeV.

A (GeV^2)	$b_{t;\text{lim}}$ (GeV^{-1})	r (fm)	x	$B(x)$
0.80	2	0.2	0.003	0.6080
0.20	4	0.4	0.01	0.5211
0.05	8	0.8	0.05	0.4655

(b) $$S_{NP}(b_T;Q) = \left[A\ln\frac{Q}{Q_{NP}} + B(x)\right]b_T^2,$$

J. Bor and D. Boer, Phys. Rev. D 106, 014030 (2022).

Approach-A

Expand $e^{-\frac{1}{2}S_A} \to 1 - S_A/2$ and coefficient fucntion $C_{g/j}$ to $\mathcal{O}(\alpha_S)$

D. Boer, U. D'Alesio, F. Murgia, C. Pisano, and P. Taels, J. High Energy Phys. 09 (2020) 040.

$$
\begin{aligned}
S_A(\boldsymbol{b}_T^2, \mu^2) &= \frac{C_A}{\pi} \int_{\mu_b^2}^{\mu^2} \frac{\mathrm{d}\bar{\mu}^2}{\bar{\mu}^2} \alpha_s(\bar{\mu}) \left(\ln \frac{\mu^2}{\bar{\mu}^2} - \frac{11 - 2n_f/C_A}{6} \right) \\
&= \frac{C_A}{\pi} \alpha_s \left(\frac{1}{2} \ln^2 \frac{\mu^2}{\mu_b^2} - \frac{11 - 2n_f/C_A}{6} \ln \frac{\mu^2}{\mu_b^2} \right).
\end{aligned}
$$

(Running of coupling is neglected)

$$
\begin{aligned}
&\hat{f}_1^g(x, b_T; \mu) \\
&= f_{g/A}(x; \mu_b) \\
&- \frac{\alpha_S}{2\pi} \left[\left(\frac{C_A}{2} \ln^2 \frac{\mu^2}{\mu_b^2} - \frac{11C_A - 2n_f}{6} \ln \frac{\mu^2}{\mu_b^2} \right) f_{g/A}(x; \mu_b) + \sum_{i=q,\bar{q},g} \int_x^1 \frac{d\hat{x}}{\hat{x}} C_{g/i}^1(x; \mu_b) f_{i/A}\left(\frac{\hat{x}}{x}; \mu_b \right) \right] e^{-S_{NP}(x, b_T)} \\
&+ \mathcal{O}(\alpha_S^2)
\end{aligned}
$$

At inpute scale, μ_b: $\quad C_{g/g}^1 = -\frac{\pi^2}{12} \delta(1-x) \qquad C_{g/q}^1 = C_{g/\bar{q}}^1 = C_F x$

Approach-A

$$\hat{h}_1^{\perp g}(x, b_T; \mu)$$
$$= \left[\frac{C_A \alpha_S(\mu_b)}{\pi} \int_x^1 \frac{\mathrm{d}\hat{x}}{\hat{x}} \left(\frac{\hat{x}}{x} - 1\right) f_{g/A}(\hat{x}, \mu_b^2) + \frac{C_F \alpha_S(\mu_b)}{\pi} \sum_{j=q,\bar{q}} \int_x^1 \frac{\mathrm{d}\hat{x}}{\hat{x}} \left(\frac{\hat{x}}{x} - 1\right) f_{j/A}(\hat{x}, \mu_b^2)\right] e^{-S_{NP}(x, b_T)} + \mathcal{O}(\alpha_S^2)$$

$$C_{g/g}^{[1]} = \frac{\alpha_s}{\pi} C_A \left(\frac{\hat{x}}{x} - 1\right),$$
$$C_{g/i=q,\bar{q}}^{[1]} = \frac{\alpha_s}{\pi} C_F \left(\frac{\hat{x}}{x} - 1\right).$$

$$S_{NP}(b_T; Q) = A \ln\left(\frac{Q}{Q_{NP}}\right) b_c^2(b_T), \qquad Q_{NP} = 1\ \mathrm{GeV}$$

$$b_c(b_T) = \sqrt{b_T^2 + \left(\frac{b_0}{Q}\right)^2} \quad \textit{and} \quad b_T^*(b_T) = \frac{b_c}{\sqrt{1 + (b_c/b_{Tmax})^2}}$$

A is fixed by defining a b_{Tlim} such that $e^{-S_{NP}}$ becomes negligible ($\sim 10^{-3}$) for a given Q

To estimate uncertainty, we consider $b_{Tlim} = 2, 4$ and $8\ \mathrm{GeV}^{-1}$

TABLE I. Value of parameter A used in $e^{-S_{NP}}$ evaluated at $Q = 4.47$ GeV.

A (GeV^2)	$b_{t;\mathrm{lim}}$ (GeV^{-1})	r (fm)
2.2697727	2	0.2
0.57415574	4	0.4
0.14395514	8	0.8

Approach-B

Perturbative tails of f_1^g and $h_1^{\perp g}$ given by integrated PDF; consider only leading order terms:

$$\hat{f}_1^g(x, b_T; \mu_0, \zeta_0) = f_{g/A}(x; \mu_0) + \mathcal{O}(\alpha_S) + \mathcal{O}(b_T\Lambda_{QCD})$$

$h_1^{\perp g}$ requires an additional gluon exchange (helicity flip); perturbative tails starts at $\mathcal{O}(\alpha_S)$

$$\hat{h}_1^{\perp g}(x, b_T; \mu_0, \zeta_0) = \frac{C_A \alpha_S(\mu_0)}{\pi} \int_x^1 \frac{\mathrm{d}\hat{x}}{\hat{x}} \left(\frac{\hat{x}}{x} - 1\right) f_{g/A}(\hat{x}, \mu_0^2) + \frac{C_F \alpha_S(\mu_0)}{\pi} \sum_{j=q,\bar{q}} \int_x^1 \frac{\mathrm{d}\hat{x}}{\hat{x}} \left(\frac{\hat{x}}{x} - 1\right) f_{j/A}(\hat{x}, \mu_0^2) + \mathcal{O}(\alpha_S) + \mathcal{O}(b_T\Lambda_{QCD})$$

Perturbative Sudakov factor S_A, as well as one-loop running of α_S; we set $\mu \sim \sqrt{\zeta} \sim Q$ and $\mu_0 \sim \sqrt{\zeta_0} \sim \mu_b$

$$S_A(b_T; Q, \mu_b) = \frac{36}{33 - 2n_f}\left[\ln\frac{Q^2}{\mu_b^2} + \ln\frac{Q^2}{\Lambda_{QCD}^2} \ln\left(1 - \frac{\ln(Q^2/\mu_b^2)}{\ln(Q^2/\Lambda_{QCD}^2)}\right) + \left(\frac{11 - 2n_f/C_A}{6}\right) \ln\left(\frac{\ln(Q^2/\Lambda_{QCD}^2)}{\ln(\mu_b^2/\Lambda_{QCD}^2)}\right)\right] + \mathcal{O}(\alpha_S^2)$$

Same for both unpol and linearly polarized TMDs

Approach-B

For semi-inclusive production of J/ψ, one also needs to include the shape function in TMD framework

This incorporates the smearing effect due to the transverse momentum of the soft gluon emitted during the formation of the bound state-also pays a role in the resummation of soft gluons

Shape functions can in general be process dependent

J. Bor and D. Boer, Phys. Rev. D 106, 014030 (2022) , D. Boer, J. Bor, L. Maxia, C. Pisano, and F. Yuan, J. High Energy Phys. 08 (2023) 105, M. G. Echevarria, J. High Energy Phys. 10 (2019) 144, S. Fleming, Y. Makris, and T. Mehen, J. High Energy Phys. 04 (2020) 122; L. Maxia, D. Boer, J. Bor 2504.19617 [hep-ph]

We have chosen an initial scale μ'_b

$$\mu_b \to \mu'_b = \frac{Qb_0}{Qb_T + b_0} \to \mu'_{b^*} = \frac{Qb_0}{Qb_T^* + b_0},$$

And a slightly different b^*_T prescription

$$b_T^*(b_T) = \frac{b_T}{\sqrt{1 + (b_T/b_{T_{\max}})^2}},$$

Ensures

$$b_T^* \le b_{T_{\max}}$$

$$\mu'_b \le Q.$$

$$S_{NP}(b_T;Q) = \left[A \ln \frac{Q}{Q_{NP}} + B(x)\right] b_T^2,$$

D. Boer and W.J. den Dunnen, Nucl. Phys. B886, 421 (2014).

Approach-A and B

$$f_1^g(x, \boldsymbol{q}_T^2, \mu) = \int_0^\infty \frac{db_T}{2\pi} b_T J_0(b_T q_T) f_1^g(x; \mu'_{b^*}) e^{-S_A(b_T^*; Q, \mu'_{b^*})} e^{-S_{NP}(b_T; Q)},$$

$$\frac{\boldsymbol{q}_T^2}{2M_p^2} h_1^{\perp g}(x, \boldsymbol{q}_T^2, \mu) = \int_0^\infty \frac{db_T}{2\pi} b_T J_2(b_T q_T) \left[\frac{\alpha_s(\mu'_{b^*})}{\pi} \int_x^1 \frac{dx'}{x'} \left(\frac{x'}{x} - 1 \right) \left\{ C_A f_1^g(x'; \mu'_{b^*}) + C_F \sum_{i=q,\bar{q}} f_1^i(x'; \mu'_{b^*}) \right\} \right] e^{-S_A(b_T^*; Q, \mu'_{b^*})} e^{-S_{NP}(b_T; Q)}.$$

Approach A : expanded the evolution kernel $e^{-1/2 S_A}$, at leading log in resummation, to fixed order in α_s and considered the perturbative part of TMDs up to $O(\alpha_s)$.
Approach B : considered only LO terms in the perturbative tails of TMDs multiplied with the evolution kernel, in the exponent only the leading order terms. Included the effect of the running of α_s.

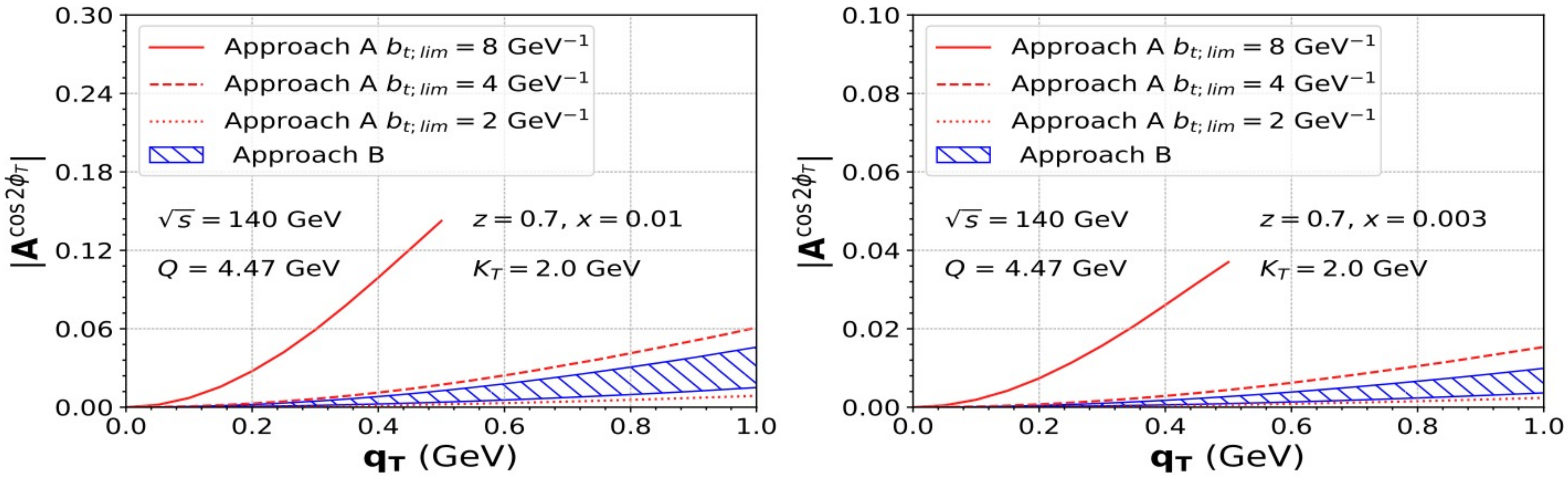

Significant different in the two approaches for larger $b_{t,lim}$: due to difference in non-perturbative factor

Band obtained by varying $b_{t,lim}$

R. Kishore, AM, A. Pawar, S. Rajesh, M. Siddiqah, PRD 111, 014003 (2025)

Numerical Results

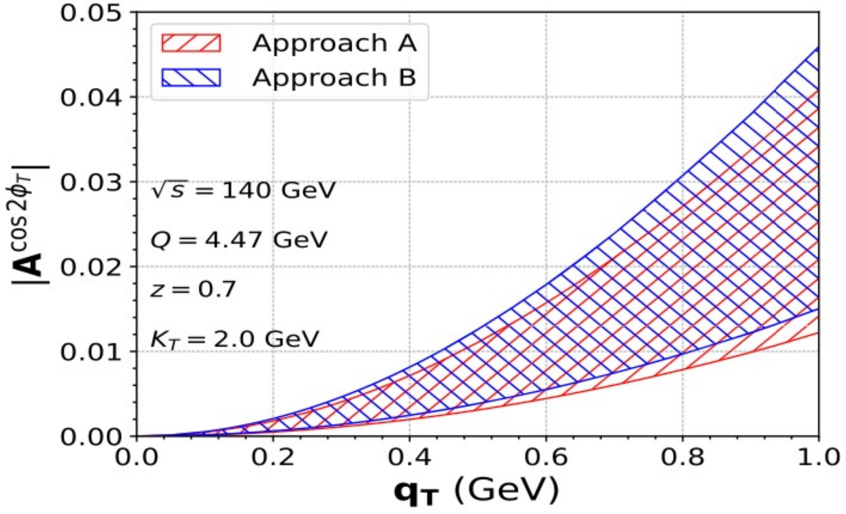

(a) x=0.01

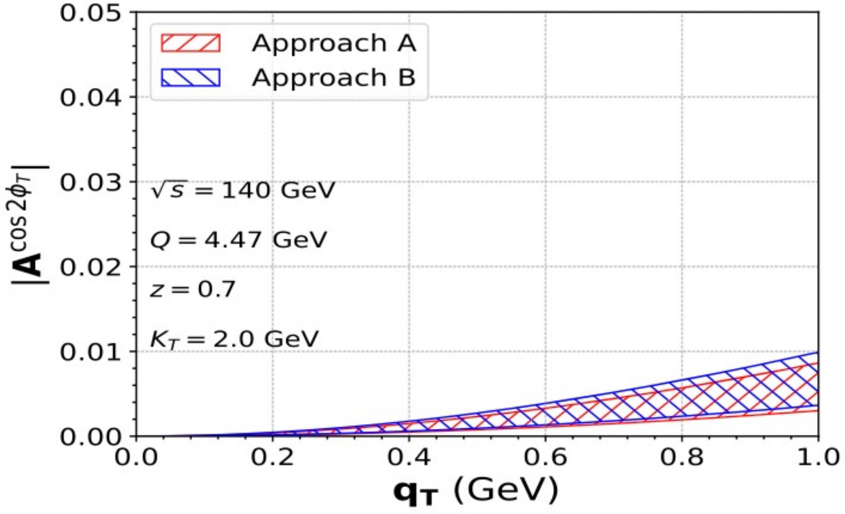

(b) x=0.003

Same non-perturbative factor

$$S_{NP}(b_T; Q) = \left[A \ln \frac{Q}{Q_{NP}} + B(x)\right] b_T^2,$$

Not so much difference between scheme A and B at low values of Q^2

Non-perturbative Sudakov factor mainly affects the asymmetry , asymmetry smaller at smaller value of x

R. Kishore, AM, A. Pawar, S. Rajesh, M. Siddiqah, PRD 111, 014003 (2025)

Numerical results

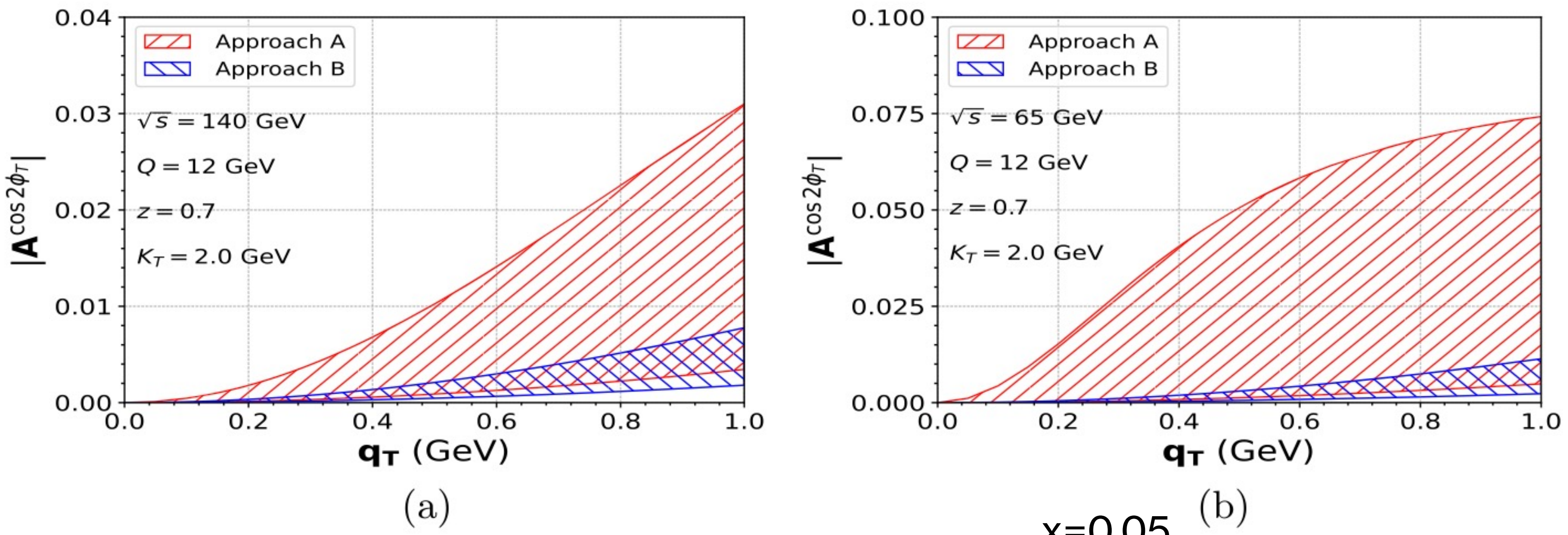

x=0.05

x=0.01

Asymmetry plotted at a higher value of Q^2 : there is significant difference between the two approaches in two different S

Asymmetries are different for larger values of $b_{t,lim}$: upper part of the band

Same non-perturbative factor

$$S_{NP}(b_T;Q) = \left[A \ln \frac{Q}{Q_{NP}} + B(x)\right] b_T^2,$$

Shows the effect of higher powers of the large logarithmic terms in the perturbative Sudakov kernel, in this kinematical region, which were not included in approach A as we expanded the exponent to a fixed order in α_s.

R. Kishore, AM, A. Pawar, S. Rajesh, M. Siddiqah, PRD 111, 014003 (2025)

Sudakov factors

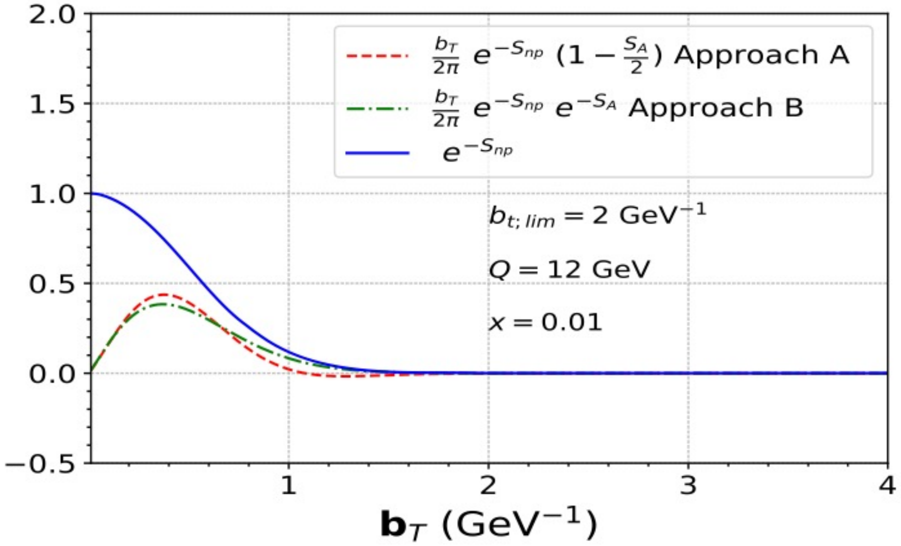

(a)

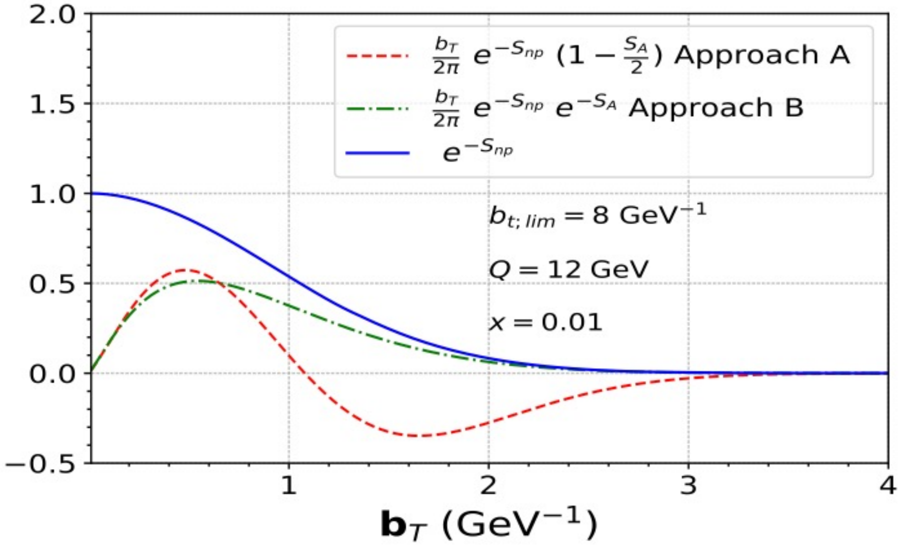

(b)

R. Kishore, AM, A. Pawar, S. Rajesh, M. Siddiqah, PRD 111, 014003 (2025)

Sudakov factors in the two approaches for two different values of $b_{t,lim}$

Same non-perturbative factor $$S_{NP}(b_T;Q) = \left[A \ln \frac{Q}{Q_{NP}} + B(x)\right] b_T^2,$$

Behaviour similar for low $b_{t,lim}$ but large logs are more pronounced when $b_{t,lim}$ is large : this causes the difference in the asymmetry

Effect of LDME set

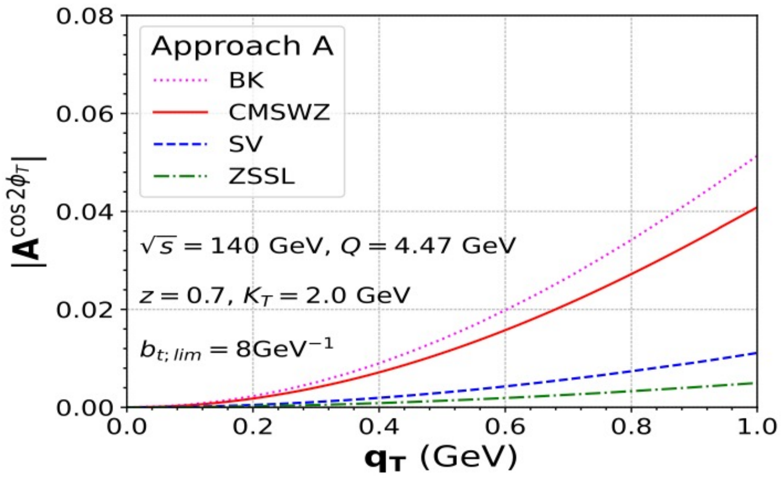

(a)

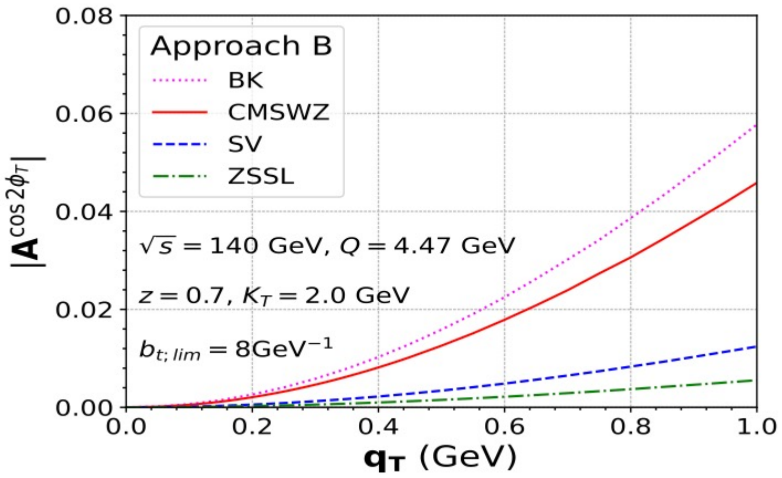

(b)

CMSWZ : K.-T. Chao, Y.-Q. Ma, H.-S. Shao, K. Wang, and Y.-J. Zhang, Phys. Rev. Lett. 108, 242004 (2012).

BK : M. Butenschön and B.A. Kniehl, Phys. Rev. Lett. 106, 022003 (2011).

SV : R. Sharma and I. Vitev, Phys. Rev. C 87, 044905 (2013).

ZSSL : Zhang, Z. Sun, W.-L. Sang, and R. Li, Phys. Rev. Lett. 114, 092006 (2015).

Uncertainty in the LDME sets introduces uncertainty in the prediction of the asymmetry

BK : gives largest asymmetry

Effect of LDME set

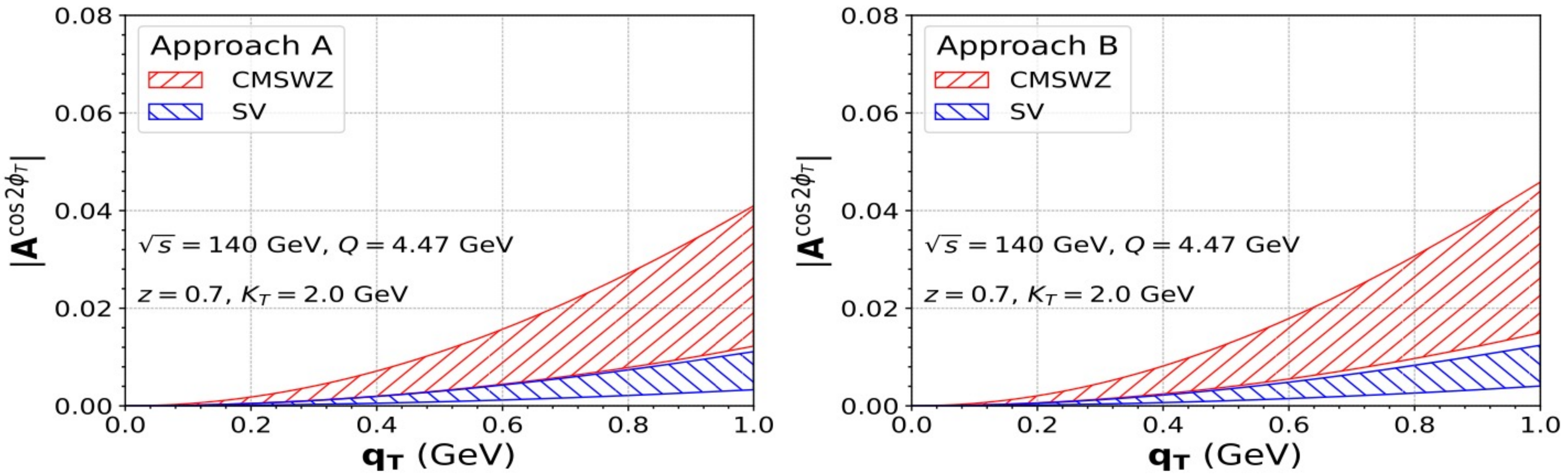

(a) (b)

Asymmetry for two different LDME sets

Uncertainty band due to the parameters also depends on the LDME set chosen. Uncertainty more for CMSWZ set

R. Kishore, AM, A. Pawar, S. Rajesh, M. Siddiqah, PRD 111, 014003 (2025)

Summary and conclusion

Presented a calculation of cos 2ϕ azimuthal asymmetry in ep -> J/ψ + jet at the EIC : useful for the extraction of linearly polarized gluon distribution

Investigated the effect of TMD evolution in detail on the asymmetry in the kinematics of EIC

Approach A : expanded the evolution kernel at leading log in resummation, to fixed order in α_s and considered the perturbative part of TMDs up to $O(\alpha_s)$.
Approach B : considered only LO terms in the perturbative tails of TMDs multiplied with the evolution kernel, in the exponent only the leading order terms. Included the effect of the running of α_s.

The non-perturbative factor for gluon TMDs is largely unknow, we investigated the effect of two different forms. Significant uncertainty band was seen in the case of S_{NP} with a larger width, allowing more contribution of the perturbative part in the higher b_T region.

We found the the perturbative part in both approaches have a similar influence on the asymmetry at a relatively low scale, but the effect is different at a larger scale,

LDMEs introduce uncertainty in the prediction of the asymmetry.